



Diversity of Haemogregarine Parasites Infecting Brazilian Anurans, with a Description of New Species of *Dactylosoma* (Apicomplexa: Adeleorina: Dactylosomatidae)

Letícia Pereira Úngari¹ · Edward Charles Netherlands² · André Luiz Quagliatto Santos³ · Edna Paulino de Alcantara¹ · Enzo Emmerich¹ · Reinaldo José da Silva¹ · Lucia Helena O'Dwyer¹

Received: 29 June 2022 / Accepted: 20 September 2022 / Published online: 20 October 2022
© The Author(s) under exclusive licence to Witold Stefański Institute of Parasitology, Polish Academy of Sciences 2022

Abstract

Purpose Brazilian anurans are considered the most diverse and species rich around the world. Although in recent years there has been a strong focus on research related to this group of animals, their parasites have not received the same attention. Thus, this study aimed to provide morphological and molecular data on haemogregarines biodiversity infecting Brazilian anurans.

Methods During 2020, 116 anurans were collected from four Brazilian States and their blood and fragment of organs were screened for haemogregarine parasites.

Results From the total, seven (6.03%) animals were found infected with species of *Hepatozoon* and *Dactylosoma*. Based on the morphological and molecular analysis, four anurans were found infected with *Hepatozoon latrensis*. The phylogenetic analysis has shown the isolates from this study grouping with the Brazilian anuran *Hepatozoon* clade, also with gene similarity ranging from 99.70 to 100% to *H. latrensis* isolates available on GenBank. Furthermore, three specimens (*Trachycephalus typhonius*, *Leptodactylus latrans*, and *Rhinella diptycha*) were infected with the same species of *Dactylosoma* (100% genetic similarity), with a genetic similarity of 98.56% to *Dactylosoma piperis* the only other species described in Brazil. In support of the molecular data, different morphological characters were observed in the blood smears as compared to *D. piperis*, suggesting that the species of *Dactylosoma* from the present study infecting three different species of Brazilian anurans is an undescribed species.

Conclusion Thus, this study increases the knowledge of Brazilian anuran blood parasites and demonstrates the importance of using integrative approaches for the diagnosis of haemoparasites.

Keywords Haemoparasite · Haemogregarine · *Hepatozoon* · Amphibian · Phylogeny · 18 S rRNA

Introduction

Amphibians are considered a diverse group of vertebrates, whose distribution extends from Tropical regions to the Arctic and North temperate zones [1]. Recently, the amphibian populations are declining around the world, due to their susceptibility of environmental pollution and emerging diseases, studies on these animals have increased, however, their parasites have not received the same attention [2, 3].

Anurans are exposed to a great variety of pathogens, and some of their blood parasites include filarial nematodes, haemoflagellates, and apicomplexans [4–6]. Intracellular haemogregarines are a diverse group of adeleorinid coccidia (Apicomplexa: Adeleorina) comprising four families: Dactylosomatidae Jakowska and Nigrelli, 1955, Haemogregarinidae Léger, 1911, Hepatozoidae Miller,

✉ Letícia Pereira Úngari
letsprungari@hotmail.com

¹ Setor de Parasitologia, DBBVPZ, Instituto de Biociências, Universidade Estadual Paulista- UNESP, Distrito de Rubião Junior, Botucatu, São Paulo, Brasil

² Department of Zoology and Entomology, University of the Free State, PO Box 339, Bloemfontein 9300, South Africa

³ Laboratório de Ensino e Pesquisa em Animais Silvestres, Faculdade de Medicina Veterinária, Universidade Federal de Uberlândia, Uberlândia, Minas Gerais, Brasil

1908, and Karyolysidae Labbé, 1894. The genus *Hepatozoon* includes the most common haemogregarines found in anurans. Several species have been described from Africa, Asia, and Europe [4, 7, 8] and according to Netherlands *et al.* [9] and Úngari *et al.* [10] there are 48 recognized species of *Hepatozoon* infecting anurans globally. In Brazil, four species of *Hepatozoon* are known, *Hepatozoon leptodactyli* (Lesage, 1908) Pessoa, 1970 described from a *Leptodactylus* sp. based solely on morphological data [11], and recently, three additional species described infecting Brazilian anurans, using morphological, morphometric and molecular tools [10].

Other haemogregarines found in anurans belong to the family Dactylosomatidae. These parasites are intracellular haemoparasites that comprises the genera *Dactylosoma* Labbé, 1894 and *Babesiosoma* Jakowska and Nigrelli, 1956. In anurans, there are only five recognised species of *Dactylosoma* [12] with *Dactylosoma piperis* Úngari, Netherlands, Silva and O'Dwyer, 2020 being currently the only species described from Brazilian anurans [12].

Due to the limited data of anuran haemogregarine parasites from Brazil, this study aimed to bring new insights on haemogregarine parasites diversity on Brazilian anurans, including a characterization of a new species of *Dactylosoma* using morphological and molecular methods.

Materials and Methods

Anuran Collection

During fieldwork in 2020, 116 anurans were collected from four Brazilian states (Mato Grosso, Mato Grosso do Sul, São Paulo, and Goiás) (Table 1). Specimens were physically restrained and the blood samples were collected by puncture of the cervical paravertebral sinus using sterile and disposable syringes and needles [13]. No ectoparasites were observed on collected animals.

After the blood collection, three thin blood smears were made on glass slides and the remaining blood sample was stored in EDTA tubes and frozen at $-10\text{ }^{\circ}\text{C}$ for further molecular analysis. All applicable international, national, and institutional guidelines for the ethical handling of animals were followed (SISBIO licence 60,640–1; CEUA-UNESP 1061).

For histological slides, the anurans were euthanized using 50 mg/kg sodium thiopental (Tiopentax[®]) administered intracerebrally, following the guidelines of Sebben [14] and the Animal Ethics Committee of Veterinary Medicine. The liver, spleen, heart, and kidney were fixed in 4% buffered neutral formalin and stained with hematoxylin–eosin [15].

Morphological Analysis

The blood smears were fixed with absolute methanol and stained with 10% Giemsa Methylene Blue Eosin Merck[®] diluted in distilled water (pH 7.0 for 50 min), according to Eisen and Schall [15]. For morphological analysis of the blood and tissue parasite stages, digital images were captured and measured using a compound microscope at 1000 \times magnification with the Leica software application suite LAS V3.8 (Leica Microsystems). Measurements are in micrometres (μm) comprising the parasite's length and width, with mean and standard deviation (means \pm standard deviation) given. Parasitaemia was calculated per 100 erythrocytes, with $\sim 10^4$ erythrocytes examined per blood smear following Cook *et al.* [16].

Molecular Analysis

DNA was extracted from whole blood samples following the blood protocol of the DNeasy Blood & Tissue Kit (Qiagen, Valencia, CA, USA). Partial 18 S rRNA gene fragments were amplified using two different pairs of primers HepF300/Hep900 (600 bp) and Hemo1/Hemo2 (900 bp) [17, 18]. The PCR amplification reactions for each pair of

Table 1 Data on Brazilian anurans collected in 2020 from Mato Grosso, Mato Grosso do Sul and São Paulo States, positives for *Hepatozoon* and *Dactylosoma* species through morphological analysis

Species	HI	Locality	Coordinates
<i>Leptodactylus labyrinthicus</i> (Spix, 1824)	<i>Hepatozoon</i>	Cocalinho city, MT	14°26'19.98"S, 51° 35'20.17"W
<i>L. labyrinthicus</i>	<i>Hepatozoon</i>	Araguaiana city, MT	14°32'13.49" S, 51°40'38.81" W
<i>Leptodactylus</i> sp.	<i>Hepatozoon</i>	Cocalinho city, MT	14°28'39.27"S, 51°36'31.95"W
<i>Rhinella mirandaribeiroi</i> (Gallardo, 1965)	<i>Hepatozoon</i>	Cocalinho city, MT	14°31'40.16"S, 51°41'34.07"W
<i>Rhinella diptycha</i> (Cope, 1862)	<i>Dactylosoma</i>	Cocalinho city, MT	14°31'10.77"S, 51°41'43.99"W
<i>Leptodactylus latrans</i> (Steffen, 1815)	<i>Dactylosoma</i>	RPPN Cisalpina city, MS	21°19'53.47"S, 51°56'39.61"W
<i>Trachycephalus typhonius</i> (Linnaeus, 1758)	<i>Dactylosoma</i>	Gavião Peixoto city, SP	21°50'43.34"S, 48°27'8.95"W

HI Hemoparasite infection, RPPN Private Reserve of Natural Heritage, MT Mato Grosso State, MS Mato Grosso do Sul State, SP São Paulo State

primers and thermocycler conditions were carried out following Úngari *et al.* [10].

PCR products were subjected to the electrophoresis at 80 V in a 1.5% agarose gel, stained with Gel Red, and observed using an ultraviolet transilluminator. The products of interest were purified by adding 2 μ L of ExoSAP-IT® (Affymetrix, Santa Clara, CA, USA) to 5 μ L of PCR product according to the manufacturer's recommendations. Amplicons were then sequenced using PCR primers on a 3500 Genetic Analyser capillary sequencer (Applied Biosystems) and after BigDye Terminator Cycle Sequencing Ready Reaction Kit v.3.1 (Applied Biosystems) according to the manufacturer's recommendations.

The sequence chromatograms obtained (forward and reverse sequences) were assembled and edited from each primer to obtain a partial 18 S rDNA consensus sequence, and then concatenated [\sim 1200 bp] using the Geneious version 7.1.3 [19] (Bomatters, www.geneious.com). Sequences from the haemogregarine group available on GenBank were aligned using Geneious version 7.1.3 [19] with MUSCLE algorithm (Bomatters, www.geneious.com). *Adelina dimidiata* Schneider, 1875, *Adelina grylli* Butaeva, 1996, and *Klossia helicina* Schneider, 1875 were selected as outgroups following Úngari *et al.* [10]. Phylogenetic relationships were inferred via Bayesian inference (BI) using MrBayes 3.2.2 [20] and Maximum likelihood (ML) analysis using RAxML 7.2.8. [21]. For the BI analysis, the Markov Chain Monte Carlo (MCMC) algorithm was run for 1 million generations, sampling every 100 generations. The first 25% of the trees were discarded as “burn-in”. The Tracer tool was used to assess convergence and the “burn-in” period [22]. For the ML analysis, nodal support was assessed using 1000 rapid bootstrap replicates [23]. The aligned sequences of haemogregarine species from anurans were compared using a pair-wise distance (p-distance) matrix.

Results

From 116 anurans screened (Table 1, Fig. 1), seven (6.03%) which correspond to three genera (*Rhinella*, *Trachycephalus* and *Leptodactylus*) and three families (Bufonidae, Hylidae and Leptodactylidae), were found infected with species of *Dactylosoma* and *Hepatozoon* based on morphological screening [10, 11, 24, 25].

A species of *Hepatozoon*, latter molecularly identified as *Hepatozoon latrensis* Úngari, Netherlands, Silva and O'Dwyer, 2021, was identified in four anurans collected at Mato Grosso State, namely two *Leptodactylus labyrinthicus*, one *Leptodactylus* sp., and one *Rhinella mirandaribeiroi* with a parasitaemia of 3.24 and 5.17%, 1.92 and 0.05% respectively. The blood smears were analysed using a light



Fig. 1 Brazilian anuran species surveyed for *Hepatozoon* and *Dactylosoma* species from this study

microscope at 100× magnification, and mature gamonts, immature gamonts, and free gamonts were observed in the peripheral blood of the four positive anurans (Fig. 2). From all the tissue fragments collected, only the spleen and liver were positive for *Hepatozoon*'s merogony; the histological slides of the four positive anurans revealed micromeronts with micromerozoites and macromeronts with macromerozoites (Fig. 3). The morphometric data are reported in Table 2.

Regarding species of *Dactylosoma*, three anurans were found positive: one *Leptodactylus latrans* from Mato Grosso do Sul State, one *Trachycephalus typhonius* from São Paulo State and one *Rhinella diptycha* from Mato Grosso State with a parasitaemia of 0.09, 0.06 and 0.16%, respectively. Based on the morphological analysis of the peripheral blood stages, it was possible to observe primary merogonic (trophozoites, early-stage meront, meronts, and merozoites) and secondary merogonic (young

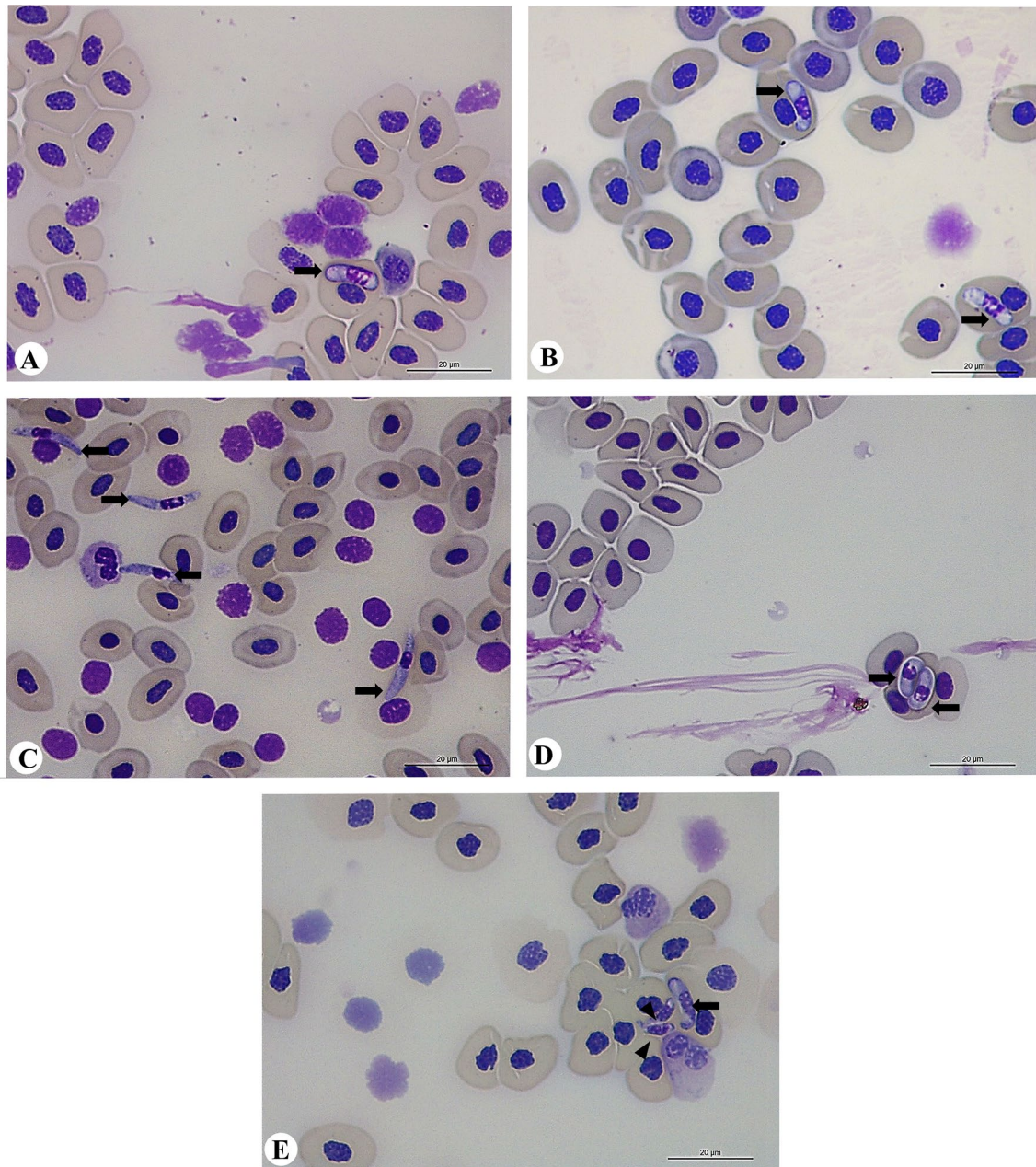


Fig. 2 A–E Morphological data on *Hepatozoon latrensis* in four anurans blood smears from Mato Grosso State, Brazil. **A** Mature gamont found in one anuran *Rhinella mirandaribeiroi* (268); **B** Mature gamont found in one *Leptodactylus labyrinthicus*; **C–D**) Free gamonts

C and mature gamonts **D** found in one *Leptodactylus* sp.; **E**–Immature (head-arrow) and mature gamonts (arrow) found in one *Leptodactylus labyrinthicus*. Scale bar: 20 µm

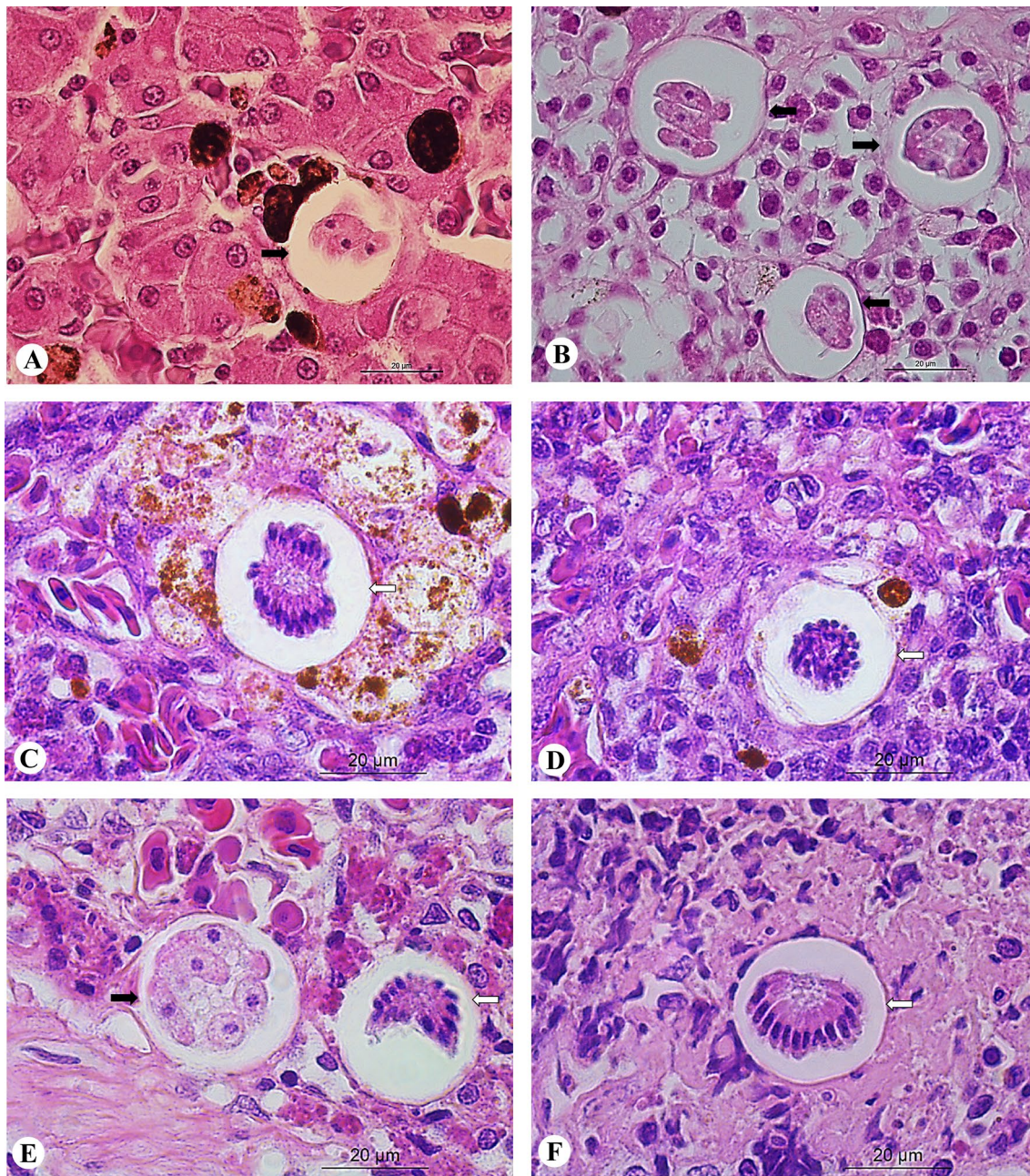


Fig. 3 A–F Histological slides containing tissue stage merogony of *Hepatozoon latrensis* in four anurans from Mato Grosso State, Brazil. **A** Trizoic cyst found in the liver of the anuran *Rhinella mirandaribeiroi*; **B** Macromeronts with macromerozoites found in the liver of *Leptodactylus labyrinthicus*; **C–D** Micromeronts with micromerozoites

found in the spleen of one *Leptodactylus* sp.; **E–F** Macromeront (**E**) and two micromeronts found in the spleen of one *Leptodactylus labyrinthicus*. Black arrow (macromeronts). White arrow (micromeronts). Scale bar: 20 µm

Table 2 *Hepatozoon* sp. measurements (mean ± standard deviation) of the blood and tissue stages from Brazilian anurans

Anuran hosts	P (%)	DS	N	C (µm)	PL (µm)	PW (µm)	PA (µm ²)	NL (µm)	NW (µm)	NA (µm ²)
<i>Rhinella mirandaribeiroi</i>	0.05	MG	20	–	12.98 ± 0.70	4.00 ± 0.10	52.37 ± 0.70	5.65 ± 0.33	4.00 ± 0.10	15.05 ± 0.32
<i>Leptodactylus labyrinthicus</i>	5.17	MG	50	–	13.10 ± 0.27	4.39 ± 0.34	52.42 ± 3.25	5.84 ± 0.50	3.60 ± 0.35	16.30 ± 1.65
		MI	1	15.68	34.97	32.31	768.15	–	–	–
		MA	6	10.95 ± 1.26	32.33 ± 1.44	33.18 ± 2.24	810.63 ± 74.36	–	–	–
		MAZ	15	–	14.79 ± 0.66	5.16 ± 0.87	67.29 ± 6.30	1.84 ± 0.49	1.65 ± 0.33	3.42 ± 0.62
		DC	1	13.18	27.21	27.60	560.85	–	–	–
		DCZ	2	–	14.74 ± 0.32	5.90 ± 0.33	66.75 ± 2.98	2.55 ± 0.28	2.35 ± 0.09	4.17 ± 0.08
		TC	2	12.59 ± 2.52	33.05 ± 1.35	30.51 ± 2.89	807.86 ± 97.13	–	–	–
		TCZ	6	–	13.70 ± 0.87	5.06 ± 0.75	62.63 ± 4.48	1.85 ± 0.50	2.19 ± 0.72	3.88 ±
<i>Leptodactylus sp.</i>	1.92	MG	50	–	11.63 ± 0.81	4.63 ± 0.49	45.97 ± 4.95	3.90 ± 0.54	3.48 ± 0.93	10.19 ± 1.92
		FG	10	–	16.61 ± 0.96	2.72 ± 0.41	39.84 ± 4.0	4.76 ± 0.64	2.39 ± 0.36	8.78 ± 1.54
		MI	3	8.02 ± 0.45	28.84 ± 1.05	29.08 ± 2.99	620.44 ± 96.43	–	–	–
		MIZ	10	–	7.06 ± 0.51	1.68 ± 0.36	12.23 ± 0.26	2.13 ± 0.95	1.24 ± 0.28	2.82 ± 0.71
		MA	2	13.67 ± 0.74	30.84 ± 0.41	34.33 ± 1.61	809.64 ± 15.69	–	–	–
		MAZ	10	–	16.53 ± 0.89	6.37 ± 0.63	87.82 ± 6.12	2.08 ± 0.45	2.42 ± 0.23	4.33 ± 0.80
		IG	50	–	9.05 ± 0.80	2.86 ± 0.33	16.92 ± 2.9	4.12 ± 0.37	2.83 ± 0.31	8.63 ± 0.60
<i>Leptodactylus labyrinthicus</i>	3.24	MG	50	–	13.09 ± 0.75	4.12 ± 0.39	47.55 ± 4.5	5.87 ± 0.84	5.92 ± 9.46	15.84 ± 3.68
		MI	11	9.25 ± 1.87	26.44 ± 1.96	26.50 ± 2.15	532.50 ± 70.75	–	–	–
		MIZ	30	–	8.13 ± 0.91	1.80 ± 0.64	14.30 ± 1.18	2.88 ± 0.67	1.41 ± 0.35	4.08 ± 0.72
		MA	12	7.85 ± 1.07	28.67 ± 3.19	27.34 ± 2.58	586.66 ± 102.10	–	–	–
		MAZ	20	–	12.46 ± 1.52	5.43 ± 0.55	58.49 ± 6.13	2.25 ± 0.43	2.28 ± 0.23	4.70 ± 0.47

P parasitaemia, C meront's capsule, N number of parasites, PL parasite length, PW Parasite width, PA Parasite area, NL Parasite nuclei length, NW Parasite nuclei width, NA Parasite nuclei area, MG Mature gamonts, IG Immature gamonts, FG free gamonts, DS Parasite's developmental stage, MI Micromeront, MA Macromeront, MAZ macromeront, DC Dizoic cyst, DCZ Dizoic cysto-
tozoite, TC Trizoic cyst, TCZ Trizoic cysto-
tozoite

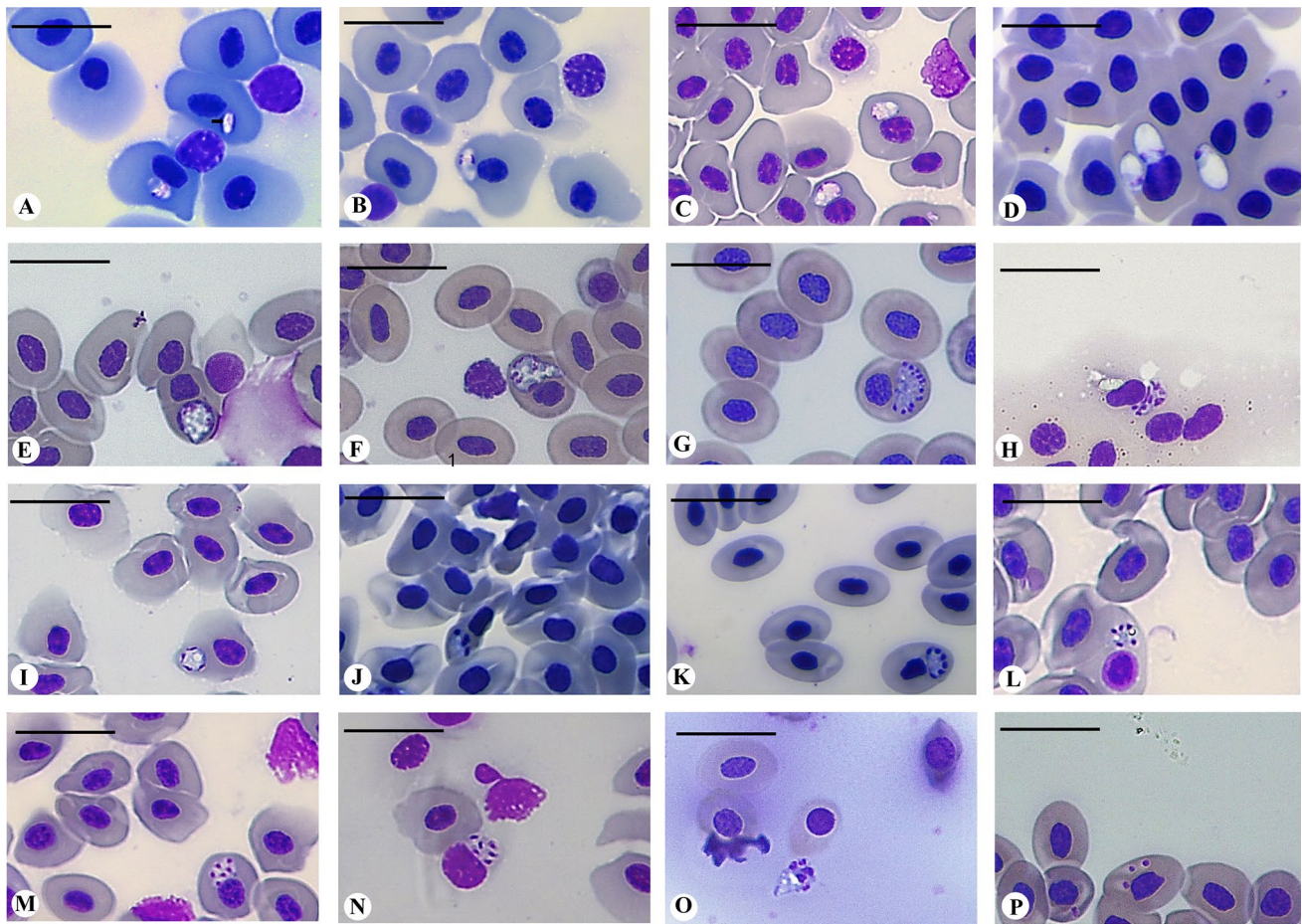


Fig. 4 A–P Morphological data on *Dactylosoma amphibia* n. sp. infecting Brazilian anurans. A–K Primary merogony: A–C Trophozoites (young trophozoite—arrow); D–E Early-stage meront; F Amoeboid appearance meront G Fan-like shaped primary meront. H Mero-

zoites. I–P Secondary merogony: I–J Young meronts; K–O Mature meronts; K Fan-like shaped meront L Meront with dactylate appearance; P Merozoites. Scale bar: 20 μ m

Table 3 *Dactylosoma amphibia* n. sp. measurements (mean \pm standard deviation) of the blood stages from Brazilian anurans

DS	N	PL (μ m)	PW (μ m)	PA (μ m ²)	NL (μ m)	NW (μ m)	NA (μ m ²)	Nu (μ m)
Primary Merogony								
Trophozoite	13	5.37 \pm 0.99	2.99 \pm 0.53	13.98 \pm 2.46	1.94 \pm 0.83	1.96 \pm 0.93	2.95 \pm 1.15	
Early-stage meront	10	6.78 \pm 0.58	3.95 \pm 0.50	19.90 \pm 3.67	2.40 \pm 1.04	2.15 \pm 0.76	2.96 \pm 1.37	
Amoeboid appearance meront	9	12.98 \pm 1.09	9.35 \pm 1.39	76.78 \pm 16.16	2.20 \pm 0.40	1.05 \pm 0.40	2.90 \pm 0.18	5–7
Fan-like shaped meront	2	10.11 \pm 0.19	7.37 \pm 0.13	58.94 \pm 1.21	0.99 \pm 0.14	0.57 \pm 0.20	0.89 \pm 0.21	13; 20
Merozoite	10	3.05 \pm 1.13	1.72 \pm 1.81	3.71 \pm 1.03	1.33 \pm 0.33	1.69 \pm 0.40	3.35 \pm 1.58	
Secondary Merogony								
Young meronts	2	5.57 \pm 0.47	4.13 \pm 1.0	16.04 \pm 1.2	0.85 \pm 0.2	0.94 \pm 0.3	2.35 \pm 0.41	3; 4
Fan-like shaped meront	2	7.01 \pm 0.22	3.99 \pm 0.14	16.98 \pm 0.52	1.15 \pm 0.24	1.02 \pm 0.07	1.59 \pm 0.71	6
Dactylate appearance meront	1	6.24	4.19	17.52	0.56 \pm 0.11	0.89 \pm 0.31	1.91 \pm 0.32	5
Mature meronts	3	10.0 \pm 0.65	6.13 \pm 1.06	42.64 \pm 5.30	1.78 \pm 0.45	1.32 \pm 0.52	2.44 \pm 1.20	5–6
Merozoites	3	5.33 \pm 0.14	4.39 \pm 0.44	17.24 \pm 0.11	2.02 \pm 0.35	1.89 \pm 0.43	4.85 \pm 1.36	

M merogony, DS Developmental stage, N number of parasites, PL parasite length, PW Parasite width, PA Parasite area, NL Parasite nuclei length, NW Parasite nuclei width, NA Parasite nuclei area, Nu nuclei

meront and meronts) developmental stages, of an unidentified species of *Datylosoma* (Fig. 4). The morphometric data are reported in Table 3.

Species Description

Datylosoma amphibia n. sp. Úngari, Netherlands, Da Silva and O'Dwyer n. sp.

Type-host: *Rhinella diptycha* [Cope, 1862] (Anura: Bufonidae).

Other hosts: *Trachycephalus typhonius* [Linnaeus, 1758] (Anura: Hylidae) and *Leptodactylus latrans* [Steffen, 1815] (Anura: Leptodactylidae).

Type-locality: Mato Grosso State (14°31'10.77"S, 51°41'43.99"W).

Other localities: *L. latrans*: Mato Grosso do Sul State (21°19'53.47"S, 51°56'39.61"W). *T. typhonius*: São Paulo State (21°50'43.34"S, 48°27'8.95"W).

Site of infection: Peripheral blood.

Prevalence: The total prevalence found was 2.58% (3/116).

Parasitaemia: 0.16%

Other parasitaemia: *L. latrans* with 0.09% and *T. typhonius* with 0.06%

Etymology: The epithet “*amphibia*” refers to the analysed host group (amphibians), since this species has low host specificity parasitizing different species of the amphibian group.

Gene sequence: The 18S rDNA gene sequences obtained were 599 bp (*R. diptycha*) [OP480618], 593 bp (*T. typhonius*) [OP480172], and 609 bp (*L. latrans*) [OP480169].

Type-material: Hapantotype 1 X blood smear from *R. diptycha* was deposited in the collection of the National Institute of Amazonian Research (INPA), Manaus, Brazil [TO BE ADDED]. Parahapantotype 2 X blood smears: 1 X from *T. typhonius* and 1X from *L. latrans* were deposited in the collection of the National Institute of Amazonian Research (INPA), Manaus, Brazil [INPA26].

Note: The authors of the new taxon are different from the authors of this paper; Article 50.1 and Recommendation 50A of the International Code of Zoological Nomenclature [26].

Morphological and Morphometric Analysis

The developmental stages of an unidentified species of *Datylosoma* were observed in three hosts, of which when the developmental stage was identified in more than one host, presented similar morphology and morphometry among them. The developmental stages observed were: trophozoites, early-stage meronts, meronts (amoeboid appearance and fan-like shaped meronts), and merozoites from primary merogony. For secondary merogony, early-stage meronts,

meronts (fan-like shaped, dactylate appearance, and round-shaped meronts), and merozoites were identified. During primary merogony, meronts producing up to 20 chromatin divisions were observed and during secondary merogony, meronts producing up to six-chromatin divisions were observed (Fig. 4, Table 3). The total number of each developmental stages found in all the positive hosts is included as the letter “n” in the end of each developmental stage description.

Primary Merogony

Trophozoite (Fig. 4A–C): small ovoid to elongated, with both extremities rounded, cytoplasmic vacuoles evidenced and cytoplasm staining whitish, measuring $5.37 \pm 0.99 \mu\text{m}$ long, $2.99 \pm 0.53 \mu\text{m}$ wide, and with area of $13.98 \pm 2.46 \mu\text{m}^2$. Nuclei not clearly defined, sometimes placed at the middle or slightly towards one end of the parasite, non-dense chromatin, and stained dark-purple, measuring $1.94 \pm 0.83 \mu\text{m}$ long, $1.96 \pm 0.93 \mu\text{m}$ wide, and with area of $2.95 \pm 1.15 \mu\text{m}^2$ ($n = 13$).

Early-stage meront (Fig. 4D–E): Ovoid shape, with large cytoplasmic vacuoles evidenced, occupying half to almost the entire parasite, dislocating towards one end of the cytoplasm and nuclear chromatin of the parasite, with the cytoplasm stained purple-bluish, measuring $6.78 \pm 0.58 \mu\text{m}$ long, $3.95 \pm 0.50 \mu\text{m}$ wide, and with area of $19.90 \pm 3.67 \mu\text{m}^2$. The nuclear chromatin in the division process stained purple, always located close to the parasite's membrane, measuring $2.40 \pm 0.37 \mu\text{m}$ long, $2.15 \pm 0.28 \mu\text{m}$ wide, and with area of $2.96 \pm 0.87 \mu\text{m}^2$. In some cases, the parasite displaced the cell nuclei towards one side causing hypertrophy of the host cell ($n = 10$).

Amoeboid shaped meront (Fig. 4F): Large meront with one end tapered and the other rounded, cytoplasm stained bluish with vacuoles always presents, measuring $12.98 \pm 1.09 \mu\text{m}$ long, $9.35 \pm 1.39 \mu\text{m}$ wide, and with area of $76.78 \pm 16.16 \mu\text{m}^2$. Multinucleate with 5–7 nuclei, non-dense nuclear chromatin distributed towards the cytoplasm stained in dark-purple, measuring $2.20 \pm 0.40 \mu\text{m}$ long, $1.05 \pm 0.40 \mu\text{m}$ wide, and with area of $2.90 \pm 0.18 \mu\text{m}^2$ ($n = 9$).

Fan-like shaped meront (Fig. 4G): Large and multinucleate meronts (13 and 20 nuclei), measuring $10.11 \pm 0.19 \mu\text{m}$ long, $7.37 \pm 0.13 \mu\text{m}$ wide, and with area of $58.94 \pm 1.21 \mu\text{m}^2$. In some cases, it is possible to observe small vacuoles in the cytoplasm, which is stained purple-bluish. Ovoid dense nuclear chromatin positioned on one side of meront, forming fan-like shape, measuring $0.99 \pm 0.14 \mu\text{m}$ long, $0.57 \pm 0.20 \mu\text{m}$ wide, and with area of $1.09 \pm 0.21 \mu\text{m}^2$. These shaped meronts always cause dislocation of the nuclei cell towards one side and, in some cases, hypertrophy of the host cell ($n = 2$).

Merozoite (H): Small, grouped together in the erythrocyte, measuring $3.05 \pm 1.13 \mu\text{m}$ long, $1.72 \pm 0.40 \mu\text{m}$ wide, and with area of $3.71 \pm 1.03 \mu\text{m}^2$. Ovoid small and dense nuclear chromatin stained dark-purple, measuring $1.33 \pm 0.33 \mu\text{m}$ long, $1.69 \pm 0.40 \mu\text{m}$ wide, and with area of $3.35 \pm 1.58 \mu\text{m}^2$ ($n = 10$).

Secondary Merogony

Early-stage meront (Fig. 4I–J): (I) Round shape with cytoplasm stained whitish, with or without small vacuoles evident, measuring $6.13 \mu\text{m}$ long, $4.09 \mu\text{m}$ wide, and with area $17.17 \mu\text{m}^2$. Multinucleate with four slender nuclei distributed peripherally with chromatin stained dark-purple, measuring $0.41 \pm 0.10 \mu\text{m}$ long, $0.78 \pm 0.32 \mu\text{m}$ wide, and with area of $1.99 \pm 0.24 \mu\text{m}^2$ ($n = 1$). (J) Elongated with one end tapered and the other rounded, with or without cytoplasmic vacuole, measuring $5.09 \mu\text{m}$ long, $4.17 \mu\text{m}$ wide, and with area of $14.91 \mu\text{m}^2$. Rounded end containing three nuclei, with dense and circular chromatin staining in deep magenta peripherally distributed, the measurements of the three nuclei are $1.15 \pm 0.2 \mu\text{m}$ long, $1.02 \pm 0.07 \mu\text{m}$ wide, and with area of $1.6 \pm 0.71 \mu\text{m}^2$ ($n = 1$).

Fan-like shaped meront (Fig. 4K): Multinucleate meront with a tapered side and the other rounded with 6 nuclei, forming fan-like shape; in some cases, it is possible to observe small cytoplasmic vacuoles, the cytoplasm stained bluish, measuring $7.01 \pm 0.22 \mu\text{m}$ long, $3.99 \pm 0.14 \mu\text{m}$ wide, and with area of $16.98 \pm 0.52 \mu\text{m}^2$. Ovoid dense chromatin positioned on one side of meront stained dark-purple, measuring $1.15 \pm 0.24 \mu\text{m}$ long, $1.02 \pm 0.07 \mu\text{m}$ wide, and with area of $1.59 \pm 0.71 \mu\text{m}^2$ ($n = 2$).

Dactylate shaped meront (Fig. 4L): Round shape (hand-like appearance) with transparent cytoplasm with or without small cytoplasmic vacuoles evidenced, measuring $6.24 \mu\text{m}$ long, $4.19 \mu\text{m}$ wide, and with area of $17.52 \mu\text{m}^2$. Multinucleate with five nuclei located peripherally with dense chromatin staining in deep magenta, with the five nuclei measuring $0.56 \pm 0.11 \mu\text{m}$ long, $0.89 \pm 0.31 \mu\text{m}$ wide, and with area of $1.91 \pm 0.32 \mu\text{m}^2$ ($n = 1$).

Mature meronts (Fig. 4M–O): Ovoid multinucleated (up to six nuclei) meronts, in some cases with one end more tapered than the other, intra or extracellular, with or without cytoplasm vacuoles; measuring $10.0 \pm 0.65 \mu\text{m}$ long, $6.13 \pm 1.06 \mu\text{m}$ wide, and with area of $42.64 \pm 5.30 \mu\text{m}^2$. Rounded to irregular shaped nuclei stained purplish, measuring $1.78 \pm 0.45 \mu\text{m}$ long, $1.32 \pm 0.52 \mu\text{m}$ wide, and with area of $2.44 \pm 1.20 \mu\text{m}^2$ ($n = 3$).

Merozoites (Fig. 4P): Small and located within the erythrocyte, with one end more tapered, measuring $5.33 \pm 0.14 \mu\text{m}$ long, $4.39 \pm 0.44 \mu\text{m}$ wide, and with area of $17.24 \pm 0.11 \mu\text{m}^2$. Rounded and dense nuclear chromatin

stained in dark-purple, measuring $2.02 \pm 0.35 \mu\text{m}$ long, $1.89 \pm 0.43 \mu\text{m}$ wide, and with area of $4.85 \pm 1.36 \mu\text{m}^2$ ($n = 3$).

Remarks Regarding morphological and morphometric data, the seven species currently recognized have their peculiarities, which proved the one described here to be a new species. Of these seven, two were described infecting fish hosts, *Dactylosoma salvelini* Fantham, Porter and Richardson, 1942 from Canada and *Dactylosoma iethrinorum* Saunders, 1960 from Egypt. The other five were described from anuran hosts: *Dactylosoma sylvatica* Fantham, Porter and Richardson, 1942 infecting *Lithobates sylvatica* LeConte, 1825 from Canada; *Dactylosoma taiwanensis* Manwell, 1964 infecting *Fejervarya limnocharis* Gravenhorst, 1829 from Taiwan; *Dactylosoma ranarum* Kruse, 1890 (syn. *D. splendens*) infecting *Pelophylax kl. esculentus* Linnaeus, 1758; *Dactylosoma kermi* Netherlands, Cook, Du Preez, Vanhove, Brendonck and Smit, 2020 infecting *Ptychadena anchietae* Bocage, 1868; *Sclerophrys gutturalis* Power, 1927 from South Africa; and *Dactylosoma piperis* Úngari, Netherlands, Silva and O'Dwyer 2020 infecting *Leptodactylus labyrinthicus* Spix, 1824 from Brazil (Table 4).

Dactylosoma amphibia n. sp. has unique characteristics that distinguish it from the seven previously described and recognized species. The first merogony is characterized by small trophozoites with cytoplasmic vacuoles, early-stage meronts with cytoplasmic vacuoles occupying almost the entire parasite, and mature meronts containing variable shapes and sizes with up to 20 nuclei per meront. Secondary merogony contained of mature meronts with up to six nuclei and free, small, and elongated intraerythrocytic merozoites. In both merogonic cycles, variable meront shape were observed, such as the fan-like, dactylate, amoeboid, and rounded shape.

According to literature, primary merogony is characterized by producing up to 16 merozoites forming a large multinucleate meront in hand-like or rosette-like shape [27]. From this study, up to 20 chromatin divisions (nuclei) in a fan-like shape and amoeboid appearance were observed. However, the second merogony is represented by up to eight merozoites [27] and in this study up to six-chromatin divisions were observed.

Netherlands *et al.* [12] reported secondary merogony of *D. kermi* with meronts producing up to six nuclei (chromatin division), similar to the present study. However, the trophozoite morphology reported in *D. kermi* can be distinguished from *Dactylosoma amphibia* n. sp. with the nuclei not evident in *D. kermi*, while in this study it was possible to identify in some cases placed at the middle or slightly towards one end of the parasite, non-dense chromatin and stained dark-purple. Moreover, *D. kermi* primary merogony

Table 4 Morphometric data on developmental stages of valid *Dactylosoma* species from fishes and anurans hosts around the world

Species	Host(s)	Country	Morphometric data (μm) ^a				Reference
			Trophozoites	Meronts (M)	Merozoites (Me)	Gametocytes	
<i>Dactylosoma salvelini</i> Fañham, Porter and Richardson, 1942	Fish <i>Salvelinus fontinalis</i> Mitch- ill, 1814	Canada	N/A	2nd M: 5.8–8.5 × 3.7–7.0	N/A	4.4–7.8 × 1.5–3.0	[39]
		Egypt	N/A	1st. M: 8.0 × 10.5	1st. M: 1.9 × 2.4	N/A	[40]
<i>Dactylosoma iethrinorum</i> Saunders, 1960	<i>Lethrinus nebulosus</i> For- sskal, 1775; <i>L. lentjan</i> Lacepède, 1802 Anuran	Canada	1st. M: 7.0–8.5 × 6.3–7.6 2nd M: 4.4 × 3.0	1st. M: 7.4–11.5 × 7.0–9.3 2nd M: 5.2 × 4.0	2nd M: 4.4–5.9 × 1.1–2.0	7.0–12.6 × 1.5–3.0	[39]
		Taiwan	1st. M: 3.9 × 7.3	2nd. M: 6.9–7.9 × 5.6–7.3	N/A	11.8–13.6 × 2.1–2.9	[41]
<i>Dactylosoma sylvatica</i> Fañham, Porter and Richardson, 1942	<i>Lithobates sylvatica</i> LeComte, 1825	Canada	1st. M: 3.0–4.0 × 1.5–2.0	1st. M: 10.0–15.0 × 2.0–3.0; 7.3 × 4.3 2 nd . M: 9.0 × 4.0; 4.7 × 3.4	1st. M: 2.8 × 0.7; 4.3 × 1.3 2 nd . M: 2.0–3.0 × 1.0–1.5; 3.4 × 0.9	5.0–8.0 × 1.5–3.0; 7.0 × 3.4	[27, 42]
		South Africa	1st. M: 5.3–7.7 × 2.6–4.4	1st. M: 8.3–12.2 × 5.1–8.0 2 nd . M: 5.6–8.6 × 4.4–6.9	1st. M: 5.0–6.6 × 1.8–3.2 2nd. M: 4.2–5.5 × 1.8–3.5	7.8–15.0 × 1.5–3.0	[12]
<i>Dactylosoma piperis</i> Ungari, Netherlands, Silva and O'Dwyer, 2020	<i>Leptodactylus labyrinthicus</i> Spix, 1824	Brazil	1st. M: 7.4 ± 1.3 × 3.75 ± 1.5	1st. M: YM: 5.2 ± 0.15 × 5.53 ± 0.7 M: 8.59 ± 0.2 × 6.73 ± 0.5 2 nd . M: YM: 6.1 ± 1.2 × 4.15 ± 0.9 QS: 7.54 ± 0.2 × 5.4 ± 0.9 FLS: 6.95 × 4.89	1st. M: 7.45 ± 0.25 × 2.90 ± 0.25 2nd. M: QS: 6.2 ± 0.2 × 1.5 ± 0.9 FLS: 5.88 ± 0.2 × 1.3 ± 0.9	N/A	[24]
		Brazil	1st. M: 5.37 ± 0.99 × 2.99 ± 0.53	1st. M: YM: 6.78 ± 0.58 × 3.95 ± 0.5 ASM: 12.98 ± 1.09 × 9.35 ± 1.39 FLS: 10.1 ± 0.19 × 7.37 ± 0.13 2nd. M: YM: 6.13 × 4.09 QS: 6.24 × 4.19 FLS: 7.01 ± 0.22 × 3.99 ± 0.14	1st. M: 3.05 ± 1.13 × 1.72 ± 0.40 2nd. M: 5.33 ± 0.14 × 4.39 ± 0.44	N/A	This study

T trophozoites, YM young meront, M meronts, Me merozoites, G gametocytes, 1st. M first merogony, 2nd. M second merogony, QS quadrangular shaped, ASM Ameboid shaped meronts, FLS fan-like shaped, N/A data not available

^aLength (mean ± standard deviation) × width (mean ± standard deviation) in micrometres (μm)

was characterized by up to 14 nuclei formed differing from this study.

Regarding *D. ranarum*, the first species in Dactylosomatidae, it has some similarities with *Dactylosoma amphibia* n. sp.; the secondary merogony of both species reported a nucleus formation stage with up to six-chromatin divisions. However, the morphometric values of *D. ranarum* are distinct in comparison with *Dactylosoma amphibia* n. sp.

Comparing the new species with *D. taiwanensis* and *D. sylvatica* different morphometric values were observed. *Dactylosoma taiwanensis* also presented square-shaped meronts and second merogony up to eight chromatin divisions, differing from this study. Moreover, only a single, most probably the secondary merogonic cycle of *D. sylvatica* is reported in the literature, with meronts only producing up to eight merozoites, differing from this study.

Regarding the only Brazilian species described so far, *D. piperis*, there are some differences observed in comparison with the species from this study. The morphometric values from both species, the number of chromatin divisions from the two merogonies, and the presence in this study of amoeboid appearance meronts from the first merogony.

Molecular and Phylogenetic Analysis:

From the seven positive specimens, four with *Hepatozoon* and three with *Dactylosoma*, seven newly generated sequences were obtained, with the species of *Dactylosoma* generating amplicons of 599 bp (OP480168), 609 bp (OP480169), and 593 bp (OP480172); and the species of *Hepatozoon* generating four concatenated sequence amplicons of 1.319 bp (OP477334); 1.365 bp (OP477337), 1359 (OP477331), and 1.391 (OP477333).

In the phylogenetic analysis based on the alignment of the SSU rRNA sequences available on GenBank, both Maximum likelihood (ML) and Bayesian inference (BI) methods reported the same topologies with supported nodes and values in the clades (Fig. 5). The trees were generated with isolates from adeleorinid parasites (Haemogregarinidae, Hepatozoidae, Karyolysidae, and Dactylosomatidae) with *Klossia helicina* (HQ224955), *Adelina dimidiata* (DQ096835), and *Adelina grylli* (DQ096836) as outgroups. From the trees, the Dactylosomatidae clade forms a sister group to the large well-supported clade comprising isolates of Haemogregarinidae, Karyolysidae, and Hepatozoidae clades. The Dactylosomatidae clade comprises only *Dactylosoma* species, of which the isolates from this study grouped close to *D. piperis* (MW264134), but in a separate branch. Regarding the large well-supported clade, the monophyletic Haemogregarinidae clade was located as a sister group of a larger-clade comprising both Karyolysidae and Hepatozoidae polyphyletic groups. Species of *Hepatozoon* isolated from large mammals formed a sister group to

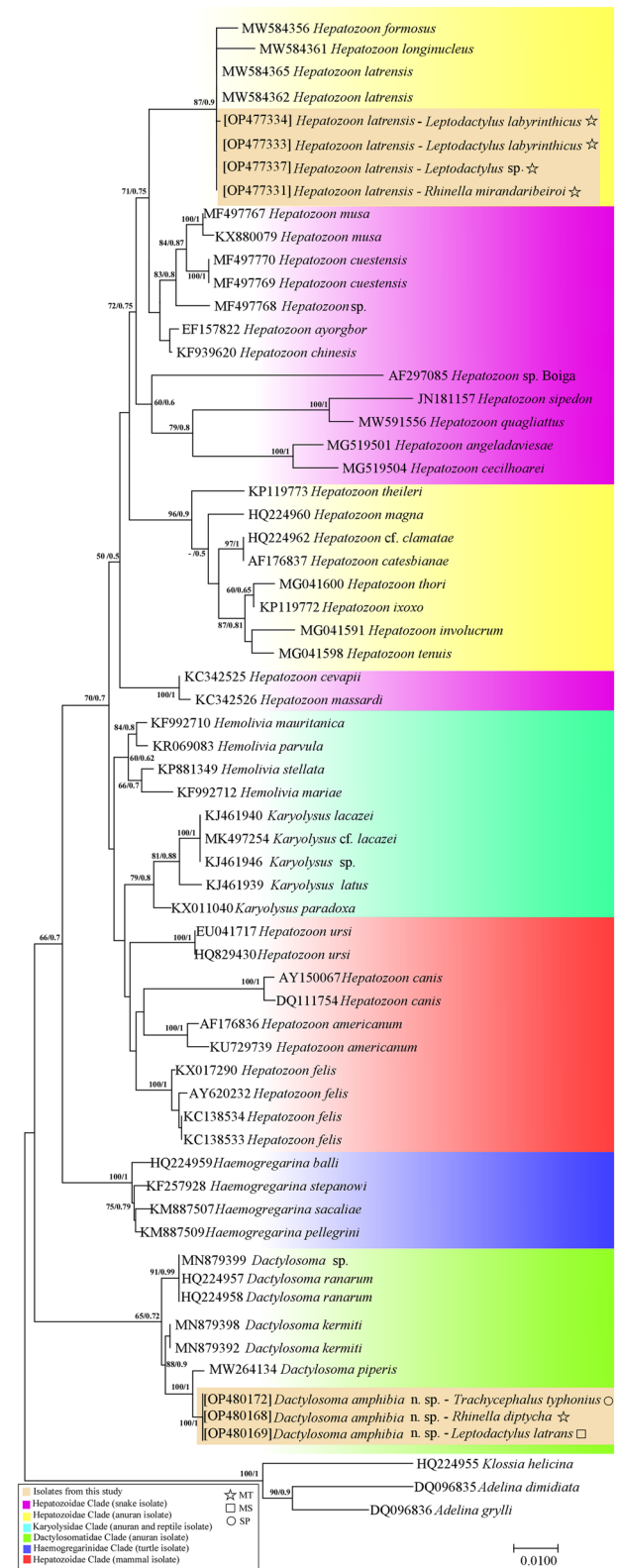


Fig. 5 Consensus phylogram of haemogregarines based on 18S rDNA sequences (486 nt). The topology trees were inferred by Bayesian (BI) and Maximum Likelihood (ML) methods (represented by ML tree). The scale bar represents 0.01 nucleotide substitutions per site. The isolates *Adelina dimidiata* (DQ096835), *Adelina grylli* (DQ096836) and *Klossia helicina* (HQ224955) were used as an out-group

the Karyolysidae clade comprising species of *Karyolysus*. Within the reptile and anuran *Hepatozoon* clade, the isolates from the present study grouped with isolates from Brazil, *H. formosus* Úngari, Netherlands, Da Silva and O'Dwyer, 2021 (MW584356), *H. longinucleus* Úngari, Netherlands, Da Silva and O'Dwyer, 2021 (MW584361), and *H. latrensis*. (MW584362/ MW584365). The isolates from Brazilian anurans formed a sister group to a clade comprising species of *Hepatozoon* from Brazilian snakes, *Hepatozoon musa* Borges-Nojosa, Borges-Leite, Maia, Zanchi-Silva, Braga and Harris, 2017 (MF497767), *Hepatozoon* sp. (MF497768), and *Hepatozoon cuestensis* O'Dwyer, Moço, Kdos, Spenasatto, da Silva and Ribolla, 2013 (MF497077).

The *Hepatozoon* isolates from the current study, were identified as *H. latrensis*, with similarity varying between 99.70–100% with *H. latrensis* (MW584365) from GenBank, with an intragenetic pair-wise divergence of 0.001 observed in the isolate OP477334 (Table 5).

Discussion

In the present study anurans of Bufonidae, Hylidae, and Leptodactylidae were screened for intracellular blood parasites, and have been found infected with *Hepatozoon latrensis* and *Dactylosoma amphibia* n. sp. Haemogregarines are considered to have a cosmopolitan distribution and have been found in all continents, except the Arctic and Antarctic regions. Some interesting questions still need to be answered regarding the evolution and dispersal of these parasites. How have they adapted to so many different host species distributed across so many varying environmental conditions and habitats? Brazilian anurans are considered a rather diverse group and more studies are required to understand their haemogregarine parasites. The present study has provided new information, helping to set a base for future work on the biodiversity of haemogregarine parasites from Brazilian anurans. Build on this knowledge will aid in answering questions on the biodiversity, evolution and dispersal of these parasites. Moreover, understanding the parasitic biodiversity and its occurrence in anurans may lead to a better comprehension of the host species condition, adaptation to the surrounding environment, and how they are affected by these parasites.

In Brazil, to date, only a handful of studies on haemogregarine parasites from anurans have been published (10, 24, 33–35). Côelho *et al.* [33] reported the occurrence of *Dactylosoma* sp. infecting four *Rhinella major* [Muller and Hellmich, 1936] with a prevalence of 5.5%, and *Rhinella marina* [Linnaeus, 1758] (the only one screened). Úngari *et al.* [24] reported on species of *Dactylosoma*, with a description of a new species, *D. piperis*, infecting one *L. labyrinthicus*. With regards to species of *Hepatozoon*, from the 145

frogs screened by Leal *et al.* [35], 18 (26.47%) *Leptodactylus chaquensis* Cei, 1950 and 24 (31.17%) *Leptodactylus podicipinus* Cope, 1862 were found parasitized. Another study from Ferreira *et al.* [34] analysed 36 anurans, and two (5.5%), one *L. latrans* and one *R. diptycha*, were infected with *Hepatozoon* sp. In addition, Úngari *et al.* [10] screened 66 anurans and reported a prevalence of 2.64% (4 host specimens) positive for species of *Hepatozoon*, two *L. latrans* and two *L. labyrinthicus*. As shown above, there have only been a few studied on haemogregarine parasites from Brazilian anurans. Furthermore, is it clear from the current data that the preevelence of haemogregarines infecting anurans from Brazil is surprisingly low. The prevalence found in the present study is 6.03%, supporting the results from similar studies conducted in Brazil [10, 33].

Four anurans were infected with *H. latrensis* in the present study. Úngari *et al.* [10] reported this parasite infecting two *L. latrans* from Mato Grosso State. Anurans of Leptodactylidae are known to harbour a great number of haemoparasites globally (30–32). Moreover, studies on haemogregarine parasites and different genera of anurans have shown more infection around anurans of the Leptodactylidae [10, 32]. According to Netherlands *et al.* [36], semi-aquatic and aquatic anurans normally show higher prevalence compared to terrestrial anurans, suggesting that the vectors may live around aquatic habitats, such as leeches. Besides, in Brazil, the first species of *Hepatozoon* described from an anuran host was *Hepatozoon leptodactyli* [Lesage, 1908] Pessoa, 1970 infecting *Leptodactylus* sp. based solely on morphological data [11]. Costa *et al.* [11] screened 90 *L. latrans* [Steffen, 1815] and *Leptodactylus pentadactylus* [Laurent, 1768] reporting 17 infected with *H. leptodactyli*. Furthermore, the leech *Haememteria lutzi* Pinto, 1920 was considered as the possible vector of *H. leptodactyli* [11]. Although the hosts from the present study were collected from the same State where *H. latrensis* was described [10], the anuran hosts were different, *R. mirandaribeiroi*, *L. labyrinthicus*, and *Leptodactylus* sp. Anurans from the Bufonidae include nocturnal and terrestrial anurans, while in the Leptodactylidae, the species were semi-aquatic and have nocturnal behaviour [11]. Leeches as possible vectors could be related to anurans of the Leptodactylidae, but are less likely for anurans from the Bufonidae, since bufonids spend time in the aquatic environment only in the breeding season, so it is more likely that possible vectors could be mosquitoes, sandflies, and other dipteran vectors [11]. Furthermore, it is important to highlight the generalist specificity of *H. latrensis*, infecting anurans from different families of Brazilian amphibians. This species has been proving how well adapted it is, infecting hosts with different ecological habits and behaviour.

To date, the complete cycle of *Dactylosoma* has not been clarified. However, Barta [43] experimentally infected

Table 5 Morphometric data on developmental stages of valid *Dactylosoma* species from fishes and anurans hosts around the world

	1	2	3	4	5	6	7	8	9	10	11	12	13	14	15	16	17	18	19	20	21	22	23	24	25
1. <i>Dactylosoma amphibibia</i> n. sp. [A309]	0.000	100	100	98.56	98.41	98.33	98.66	98.66	98.66	98.50															
2. <i>Dactylosoma amphibibia</i> n. sp. [A243]	0.000	0.000	100	98.56	98.40	98.31	98.65	98.65	98.48																
3. <i>Dactylosoma amphibibia</i> n. sp. [A261]	0.006	0.006	0.006	0.006	0.006	0.006	0.006	0.006	0.006																
4. <i>D. piperis</i> [MW264134]	0.016	0.016	0.015	0.016	0.016	0.015	0.015	0.015																	
5. <i>D. ranarum</i> [HQ224958]	0.017	0.017	0.017	0.017	0.017	0.017	0.017	0.017																	
6. <i>D. ranarum</i> [HQ224957]	0.014	0.014	0.013	0.014	0.014	0.013	0.013	0.013																	
7. <i>D. kermiiti</i> [MN879398]	0.014	0.014	0.013	0.014	0.014	0.013	0.013	0.013																	
8. <i>D. kermiiti</i> [MN879392]	0.016	0.016	0.015	0.016	0.016	0.015	0.015	0.015																	
9. <i>Dactylosoma</i> sp. [MN879399]																									
10. <i>H. latrensis</i> [A319]																									
11. <i>H. latrensis</i> [A268]										99.70	99.71	99.71	99.71	99.71	99.70	98.12	98.55	95.71	95.07	95.67	95.75	95.60	95.06	95.31	94.34
12. <i>H. latrensis</i> [A299]										0.001	100	100	100	100	100	98.40	98.83	95.88	95.28	95.84	95.92	95.77	95.28	95.47	94.53
13. <i>H. latrensis</i> [A313]										0.001	0.000	100	100	100	100	98.40	98.83	95.88	95.28	95.84	95.92	95.77	95.36	95.52	94.64
14. <i>H. latrensis</i> [MW584365]										0.001	0.000	0.000	100	100	100	98.40	98.83	95.88	95.28	95.84	95.92	95.77	95.36	95.52	94.64
15. <i>H. latrensis</i> [MW584362]										0.001	0.000	0.000	0.000												
16. <i>H. longinucleus</i> [MW584361]										0.005	0.002	0.013	0.013	0.013	0.013										
17. <i>H. formosus</i> [MW584356]										0.002	0.041	0.004	0.004	0.004	0.004										
18. <i>H. magna</i> [HQ224960]										0.005	0.051	0.040	0.041	0.041	0.041										
19. <i>H. theileri</i> [KP119773]										0.041	0.043	0.049	0.050	0.050	0.050										
20. <i>H. thori</i> [MG041600]										0.051	0.042	0.042	0.042	0.042	0.042										

Table 5 (continued)

	1	2	3	4	5	6	7	8	9	10	11	12	13	14	15	16	17	18	19	20	21	22	23	24	25
21. <i>H. renais</i> [MG041598]										0.043	0.044	0.041	0.041	0.041											
22. <i>H. involucrium</i> [MG041591]										0.042	0.051	0.043	0.043	0.043											
23. <i>H. ixoro</i> [KP119772]										0.044	0.047	0.050	0.050	0.050											
24. <i>H. cf. clamatae</i> [HQ224962]										0.051	0.056	0.046	0.046	0.046											
25. <i>H. catesbianae</i> [AF176837]										0.047	0.000	0.055	0.055	0.055											

Desserobdella picta (Verrill, 1872), the natural vector of *B. stableri*, with *D. ranarum* using frogs captured on the French island of Corsica. Although there was no development of zygote formation or gametes, it was observed *D. ranarum* sporogonic formation in the intestinal epithelium of the experimentally infected leech host (Barta, 1991). Moreover, Nöller [44] was the first to attempt transmission of *D. ranarum* using the leech *Hemiclepsis margmata* (Müller, 1774), but failed despite repeated attempts. In another study, Boulard *et al.* [45] tested *Culicoides nubeculosus* (Meigen, 1830) mosquitoes as a potential vector of *D. ranarum*, but the experiments were inconclusive. Therefore, studies aimed at possible vectors of *Dactylosoma* were developed experimentally. Future studies should be done emphasizing life cycles, with possible vectors captured in their environment, enriching the poor knowledge about *Dactylosoma* life cycles.

Regarding the morphological data, *H. latrensis* from this study presented some new developmental stages in blood smears, with free gamonts and microgamonts reported for the first time. Moreover, through molecular analysis, it was possible to identify the haemoparasites species found in this study, and also aid in the description of an undescribed species. Thus, the usefulness of molecular analysis as a diagnostic tool is shown in this study. Moreover, although the molecular tool provides inferences about species description, only by integrating the techniques of morphology, morphometry and molecular analysis, we can have advances in species description and how these parasites behave in different hosts.

These biodiversity of parasites infecting anurans only shows how important it is study this group of animals, of which is experiencing large-scale declines in species diversity. Over the last years, a third of the estimated amphibian species have declined, according to the IUCN Global Amphibian Assessment [28]. Nowadays, 8,425 anuran species have been described around the world, with a notable number of 1,146 Brazilian species [29]. Therefore, since anurans are known to harbour a great number of haemoparasites, with haemogregarines being the most commonly reported [30–32], this study has its relevancy for science, increasing the knowledge of parasites biodiversity.

Conclusion

The number of studies focussing on amphibian has been increasing in recent years, due to the possible extinction of this group [1]. However, in Brazil, the richest country in amphibian diversity, studies on parasites have not received the same attention, even with researches showing that parasites directly influence their quality of life, behaviour, reproduction, fecundity, fitness, and reproduction [32, 37, 38].

Thus, the first step for a better comprehension of host-parasite relation, potential pathogenicity, and their consequences for the anuran hosts is the correct identification of these parasites. Based on the information reported above, our study contributes to reducing the lack of knowledge on haemogregarine biodiversity infecting Brazilian anurans from the Midwest and Southeast regions, and includes the description of a new species of *Dactylosoma*, *Dactylosoma amphibia* n. sp., through morphological, morphometric and molecular approaches.

Acknowledgements We thank the team of the Laboratory for Teaching and Research in Wild Animals (LAPAS) and Non-governmental organization for the preservation of wild animals in Brazil (ONG PAS). Financial assistance: R.J.S. is supported by FAPESP (2016/50377-1); CNPq (309125/2017-0); CNPq-PROTAX (440496/2015-2). L.P.U is supported by FAPESP (2018/00754-9; 2018/09623-4). L.H.O is supported by FAPESP (2018/09623-4).

Declarations

Conflict of Interest The authors declare that they have no conflict of interest.

Ethical Standards All applicable international, national and/or institutional guidelines for the care and use of animals were followed (IBAMA licence 60640–1; CEUA-UNESP 1061).

References

- Wake D, Vredenburg VT (2008) Are we in the midst of the sixth mass extinction? A view from the world of amphibians. *Proc Natl Acad Sci USA* 105:11466–11473. <https://doi.org/10.1073/pnas.0801921105>
- Isaak-Delgado AB, López-Díaz O, Romero-Callejas E, Martínez-Hernández F, Muñoz-García CI, Villalobos G, Randón-Franco E (2020) Morphological and molecular characteristics of hemoparasites in vaillant's frogs (*Lithobates vaillanti*). *Parasitol Res* 119:1891–1901. <https://doi.org/10.1007/s00436-020-06689-1>
- Stuart S, Chanson J, Cox N, Young B (2006) El estado global de los anfibios. In: Ângulo A, Rueda J, Rodríguez J, La Marca E (eds) Técnicas de inventario y monitoreo para los anfibios de la región tropical andina. Conservación internacional serie manuales para la conservación, vol 2. Panamericana Formas e Impresos S A, Bogotá, pp 19–34
- Netherlands EC, Cook CA, Smit NJ (2014) *Hepatozoon* species [Adeleorina: Hepatozoidae] of African bufonids, with morphological description and molecular diagnosis of *Hepatozoon ixoxo* sp. nov. parasitising three *Amietophrynus* species (Anura: Bufonidae). *Parasit Vectors* 7:552–563. <https://doi.org/10.1186/s13071-014-0552-0>
- Barta JR, Ogedengbe JD, Martin DS, Smith TG (2012) Phylogenetic position of the Adeleorinid Coccidia (Myxozoa, Apicomplexa, Coccidia, Eucoccidiorida, Adeleorina) inferred using 18S rDNA sequences. *J Eukaryot Microbiol* 59:171–180. <https://doi.org/10.1111/j.1550-7408.2011.00607.x>
- Davies A, Johnston M (2000) The biology of some intraerythrocytic parasites of fishes, Amphibia and reptiles. *Adv Parasitol* 45:1–107. [https://doi.org/10.1016/S0065-308X\(00\)45003-7](https://doi.org/10.1016/S0065-308X(00)45003-7)
- Netherlands EC, Cook CA, Smit NJ, Du Preez LH (2014) Redescription and molecular diagnosis of *Hepatozoon theileri* (Laveran, 1905) (Apicomplexa: Adeleorina: Hepatozoidae) infecting *Amietia queketti* (Anura: Pyxicephalidae). *Folia Parasitol* 61:239–300. <https://doi.org/10.14411/fp.2014.046>
- Levine ND (1988) The protozoan phylum apicomplexan, vol 2. CRC Press, Boca Raton
- Netherlands EC, Cook CA, Du Preez LH (2018) Monophyly of the species of *Hepatozoon* (Adeleorina: Hepatozoidae) parasitising (African) anurans, with the description of three new species from hyperoliid frogs in South Africa. *Parasitol* 145:1039–1050. <https://doi.org/10.1017/S003118201700213X>
- Úngari LP, Netherlands EC, Santos ALQ, Alcantara EP, Emmerich E, Silva RJ, O'Dwyer LH (2021) New insights on the diversity of Brazilian anuran blood parasites: with the description of three new species of *Hepatozoon* (Apicomplexa:Hepatozoidae) from Leptodactylidae anurans. *Int J Parasitol* 14:190–201. <https://doi.org/10.1016/j.ijppaw.2021.02.009>
- Costa SCG, Pessoa SB, Pereira NM, Colombo T (1973) The life history of *Hepatozoon leptodactyli* (Lesage, 1908) Pessoa, 1970: a parasite of the common laboratory animal – the frog of the genus *Leptodactylus*. *Mem Inst Oswaldo Cruz* 71:1–18. <https://doi.org/10.1590/S0074-02761973000100001>
- Netherlands EC, Cook CA, Du Preez LH, Vanhove MPM, Brendonck L, Smit NJ, (2020) An overview of the Dactylosomatidae (Apicomplexa: Adeleorina: Dactylosomatidae), with the description of *Dactylosoma kermitti* n. sp. parasitising *Ptychadena anchietae* and *Sclerophrys gutturalis* from South Africa. *Int J Parasitol* 11:246–260. <https://doi.org/10.1016/j.ijppaw.2019.12.006>
- Zippel KC, Lillywhite HB, Mladinich CR (2001) New vascular system in reptiles: anatomy and postural hemodynamics of the vertebral venous plexus in snakes. *J Morphol* 250:173–184. <https://doi.org/10.1002/jmor.1063>
- Sebben A (2007) Microdissecção fisiológica a fresco: uma nova visão sobre a anatomia de anfíbios e répteis. In: Nascimento LB, Oliveira ME (eds) Herpetologia no Brasil, vol 2. Sociedade Brasileira de Herpetologia, Belo Horizonte, pp 311–325
- Eisen RJ, Schall JJ (2000) Life history of malaria parasite (*Plasmodium mexicanum*): independent traits and basis for variation. *Proc R Soc B: Biol Sci* 267:793–799. <https://doi.org/10.1098/rspb.2000.1073>
- Cook CA, Smit NJ, Davies AJ (2009) A redescription of *Haemogregarina fitzsimonsi* Dias, 1953 and some comments on *Haemogregarina parvula* Dias, 1953 (Adeleorina: Haemogregarinidae) from Southern African tortoises (Cyrtodira: Testudinidae) with new host data and distribution records. *Folia Parasitol* 56:173–179. <https://doi.org/10.14411/fp.2009.021>
- Ujvari B, Madsen T, Olsson M (2004) High prevalence of *Hepatozoon* spp. (Apicomplexa, Hepatozoidae) infection in water pythons (*Liasis fuscus*) from Tropical Australia. *J Parasitol* 90:670–672. <https://doi.org/10.1645/GE-204R>
- Perkins SL, Keller AK (2001) Phylogeny of nuclear small subunit rRNA genes of hemogregarines amplified with specific oligonucleotides. *J Parasitol* 87:870–876. [https://doi.org/10.1645/0022-3395\(2001\)087\[0870:PONSSR\]2.0.CO;2](https://doi.org/10.1645/0022-3395(2001)087[0870:PONSSR]2.0.CO;2)
- Kearse M, Moir R, Wilson A, Stones-Havas S, Cheung M, Sturrock S, Buxton S, Cooper A, Markowitz S, Duran C, Thierer T, Ashton B, Meintjes P, Drummond A (2012) Geneious basic: an integrated and extendable desktop software platform for the organization and analysis of sequence data. *Bioinformatics* 28:1647–1649. <https://doi.org/10.1093/bioinformatics/bts199>
- Huelsensbeck JP, Ronquist F (2001) MRBAYES: Bayesian inference of phylogenetic trees. *Bioinformatics* 17:754–755. <https://doi.org/10.1093/bioinformatics/btg180>

21. Stamatakis A (2014) RAxML version 8: a tool for phylogenetic analysis and post-analysis of large phylogenies. *Bioinformatics* 30:312–313. <https://doi.org/10.1093/bioinformatics/btu033>
22. Rambaut A, Drummond AJ, Xie D, Baele G, Suchard MA (2018) Posterior summarisation in Bayesian phylogenetics using Tracer 1.7. *Syst Biol* 67:901–904. <https://doi.org/10.1093/sysbio/syy032>
23. Rambaut A (2012) FigTree v1.4.2. Available at: <http://tree.bio.ed.ac.uk/software/figtree/> (Accessed Mar 2022).
24. Úngari LP, Netherlands EC, Santos ALQ, Alcantara EP, Emmerich E, Silva RJ, O'Dwyer LH (2020) A new species, *Dactylosoma piperis* n. sp. (Apicomplexa, Dactylosomatidae), from the pepper frog *Leptodactylus labyrinthicus* (Anura, Leptodactylidae) from Mato Grosso State, Brazil. *Parasite* 27:73. <https://doi.org/10.1051/parasite/2020070>
25. O'Dwyer LH, Moço TC, Paduan KS, Spenassatto C, Silva RJ, Ribolla PE (2013) Description of three new species of *Hepatozoon* (Apicomplexa, Hepatozoidae) from Rattlesnakes (*Crotalus durissus terrificus*) based on molecular, morphometric and morphologic characters. *Exp Parasitol* 135:200–207. <https://doi.org/10.1016/j.exppara.2013.06.019>
26. ICZN, International Code of Zoological Nomenclature (1999) The International Trust for Zoological Nomenclature: London. Available at: <http://www.nhm.ac.uk/hosted-sites/iczn/code/> (Accessed July 2021).
27. Barta JR, Boulard Y, Desser SS (1987) Ultrastructural observations on secondary merogony and gametogony of *Dactylosoma ranarum* Labbé, 1894. *J Parasitol* 73:1019–1029. <https://doi.org/10.2307/3282527>
28. Frost DR (2019) Amphibian species of the world. American Museum of Natural History, New York
29. Frost DR (2022) Amphibian species of the world: an online reference. American Museum of Natural History, New York
30. Telford SR Jr (2009) Hemoparasite of the reptilian: color atlas and text. CRC Press, Boca Raton
31. Smith TG (1996) The genus *Hepatozoon* (Apicomplexa: Adeleorina). *J Parasitol* 82:565–585. <https://doi.org/10.2307/3283781>
32. Barta JR, Desser SS (1984) Blood parasites of amphibians from Algonquin Park, Ontario. *J Wildl Dis* 20:180–189. <https://doi.org/10.7589/0090-3558-20.3.180>
33. Côelho TA, De Souza DC, Oliveira EC, Correa LL, Viana LA, Kawashita-Roberto RC (2021) Haemogregarine of Genus *Dactylosoma* (Adeleorina: Dactylosomatidae) in species of *Rhinella* (Anura: Bufonidae) from the Brazilian Amazon. *Acta Parasitol* 66:1574–1580. <https://doi.org/10.1007/s11686-021-00399-z>
34. Ferreira DAR, Perles L, Machado RZ, Prado CPA, André MR (2020) Molecular detection of Apicomplexan hemoparasites in anurans from Brazil. *Parasitol Res* 119:3469–3479. <https://doi.org/10.1007/s00436-020-06835-9>
35. Leal DDM, Dreyer CS, Da Silva RJ, Ribolla PEM, Paduan KS, Blanchi I, O'Dwyer LH, (2015) Characterization of *Hepatozoon* spp. in *Leptodactylus chaquensis* and *Leptodactylus podicipinus* from two regions of the Pantanal, state of Mato Grosso do Sul, Brazil. *Parasitol Res* 114:1541–1549. <https://doi.org/10.1007/s00436-015-4338-x>
36. Netherlands EC, Cook CA, Du Kruger DJD, Du Preez LH, Smit NJ (2015) Biodiversity of frog haemoparasites from sub-tropical northern KwaZulu-Natal. South Africa. *IJP:PAW* 4:135–141. <https://doi.org/10.1016/j.ijppaw.2015.01.003>
37. Segalla M, Berneck B, Canedo C, Caramaschi U, Cruz CAG, Garcia PCA, Grant T, Haddad CFB, Lourenço AC, Mangia S, Mott T, Nascimento L, Toledo LF, Werneck F, Langone LA (2021) List of Brazilian amphibians. *Herpetol Bras* 10:121–216. <https://doi.org/10.5281/zenodo.4716176>
38. Lainson R, Paperna I, Naiff RD (2003) Developmental of *Hepatozoon caimani* (Carini, 1909) Pessoa, de Biasi and Souza, 1972 in the caiman *Caiman c. crocodilus*, the frog *Rana catesbiana* and the mosquito *Culex fatigans*. *Mem Inst Oswaldo Cruz* 98:103–113
39. Fantham HB, Porter A, Richardson LR (1942) Some haematozoa observed in vertebrates in Eastern Canada. *Parasitology* 34:199–226. <https://doi.org/10.1017/S0031182000016176>
40. Saunders DC (1960) A survey of the blood parasites in the fishes of the Red Sea. *Trans Am Micros Soc* 79:239–252. <https://doi.org/10.2307/3223730>
41. Manwell RD (1964) The genus *Dactylosoma*. *J Protozool* 11:526–530. <https://doi.org/10.1111/j.1550-7408.1964.tb01792.x>
42. Kruse W (1890) Archiv für pathologische. *Anatomie Physiol für klin Med* 120:173–183
43. Barta JR (1991) The dactylosomatidae. *Adv Parasitol* 30:1–37
44. Nöller W (1913) Die Blutprotozoen des wasserfrosches und ihre übertragung. *Archiv für Protistenkunde* 31:169–240
45. Boulard Y, Vivier E, Landau I (1982) Ultrastructure de *Dactylosoma ranarum* (Kruse, 1890); affinités avec les coccidies; révision du statut taxonomique des dactylosomides. *Protistologica* 18:103–112

Publisher's Note Springer Nature remains neutral with regard to jurisdictional claims in published maps and institutional affiliations.

Springer Nature or its licensor holds exclusive rights to this article under a publishing agreement with the author(s) or other rightsholder(s); author self-archiving of the accepted manuscript version of this article is solely governed by the terms of such publishing agreement and applicable law.